Supplemental Material for "Precise Quantum Control of Molecular Rotation Toward a Desired Orientation"

Qian-Qian Hong,[1] Daoyi Dong,[2] Niels E. Henriksen,[3]

Franco Nori,[4,5] Jun He,[1,*] and Chuan-Cun Shu[1,†]

[1]*Hunan Key Laboratory of Nanophotonics and Devices,*

Hunan Key Laboratory of Super-Microstructure and Ultrafast Process,

School of Physics, Central South University, Changsha, 410083, China

[2]*Australian Artificial Intelligence Institute,*

Faculty of Engineering and Information Technology,

University of Technology Sydney, NSW 2007, Australia

[3]*Department of Chemistry, Technical University of Denmark,*

Building 207, DK-2800 Kongens Lyngby, Denmark

[4]*Quantum Computing Center and Theoretical Quantum*

Physics Laboratory, RIKEN, Saitama 351-0198, Japan

[5]*Physics Department, University of Michigan, Ann Arbor, Michigan 48109, USA*

Abstract

This supplementary material provides detailed derivations for obtaining the general solution of the time-dependent wave function of a molecule subjected to a pulse sequence composed of multiple sub-pulses, starting from its rotational and vibrational ground state within the ground electronic state. It explores the theoretical maximum degrees of orientation by varying the number of rotational states. It also investigates the impact of pulse duration on molecular orientation. Furthermore, it showcases a further application of this analytical approach to polyatomic nonlinear molecules.

I. AN ANALYTICAL SOLUTION FOR THE TIME-DEPENDENT WAVE PACKET

In this section, we delve into a more detailed explanation of the derivation process for the time-dependent wave function. As illustrated in Figure 1 in the main text, each subpulse $E_n(t)$ independently excites two adjacent states, denoted as $|J-1\rangle$ and $|J\rangle$ ($n = J$). Expanding the unitary time-evolution operator to include the first-order Magnus term in the interaction picture, we can express the wave function of the two-level subsystem as

$$|\psi^n(t)\rangle = \left\{ \cos\theta_n(t) |J-1\rangle\langle J-1| + i\sin\theta_n(t)\exp\left[-i(\phi_n - \omega_{n,n-1}\tau_n)\right]|J\rangle\langle J-1| \right\}\left|\psi^{n-1}(t)\right\rangle, \quad \text{(S1)}$$

where $\left|\psi^0(t)\right\rangle = |0\rangle$ is the initial wave function of the molecule without pulse driving. After a single pulse ($N = 1$) excitation, the time-dependent wave function of the molecule reads

$$|\psi(t)\rangle_1 = \cos\theta_1(t)|0\rangle + i\sin\theta_1(t)\exp\left[-i(\phi_1 - \omega_{1,0}\tau_1)\right]|1\rangle. \quad \text{(S2)}$$

In the case of $N = 2$, we have

$$|\psi(t)\rangle_2 = \cos\theta_1(t)|0\rangle + \left\{ \cos\theta_2(t)|1\rangle + i\sin\theta_2(t)\exp\left[-i(\phi_2 - \omega_{2,1}\tau_2)\right]|2\rangle \right\}\times$$
$$i\sin\theta_1(t)\exp\left[-i(\phi_1 - \omega_{1,0}\tau_1)\right]. \quad \text{(S3)}$$

For a pulse sequence comprising three subpulses ($N = 3$), the time-dependent wave function can be represented as

$$|\psi(t)\rangle_3 = \cos\theta_1(t)|0\rangle + \cos\theta_2(t)i\sin\theta_1(t)\exp\left[-i(\phi_1 - \omega_{1,0}\tau_1)\right]|1\rangle$$
$$+ \left\{ \cos\theta_3(t)|2\rangle + i\sin\theta_3(t)\exp\left[-i(\phi_3 - \omega_{3,2}\tau_3)\right]|3\rangle \right\}\times \quad \text{(S4)}$$
$$i\sin\theta_1(t)\exp\left[-i(\phi_1 - \omega_{1,0}\tau_1)\right]i\sin\theta_2(t)\exp\left[-i(\phi_2 - \omega_{2,1}\tau_2)\right].$$

* junhe@csu.edu.cn

† cc.shu@csu.edu.cn

Considering that the molecule is driven by four subpulses ($N = 4$), we can express the wave function as

$$
\begin{aligned}
|\psi(t)\rangle_4 = {} & \cos\theta_1(t)\,|0\rangle + \cos\theta_2(t) i \sin\theta_1(t) \exp\left[-i(\phi_1 - \omega_{1,0}\tau_1)\right] |1\rangle \\
& + \cos\theta_3(t) i \sin\theta_1(t) \exp\left[-i(\phi_1 - \omega_{1,0}\tau_1)\right] i \sin\theta_2(t) \exp\left[-i(\phi_2 - \omega_{2,1}\tau_2)\right] |2\rangle \\
& + \left[\cos\theta_4(t)\,|3\rangle + i \sin\theta_4(t) \exp\left[-i(\phi_4 - \omega_{4,3}\tau_4)\right] |4\rangle \right] i \sin\theta_1(t) \exp\left[-i(\phi_1 - \omega_{1,0}\tau_1)\right] \\
& \times i \sin\theta_2(t) \exp\left[-i(\phi_2 - \omega_{2,1}\tau_2)\right] i \sin\theta_3(t) \exp\left[-i(\phi_3 - \omega_{3,2}\tau_3)\right].
\end{aligned}
\tag{S5}
$$

As a result, the general solution of the time-dependent wave function after a pulse sequence consisting of N subpulses can be expressed as

$$
\begin{aligned}
|\psi(t)\rangle_N = {} & \cos\theta_1(t)\,|0\rangle + \sum_{J=1}^{N-1}\cos\theta_{J+1}(t) \prod_{n=1}^{J} i \sin\theta_n(t) \exp\left[-i(\phi_n - \omega_{n,n-1}\tau_n)\right] |J\rangle \\
& + \prod_{n=1}^{N} i \sin\theta_n(t) \exp\left[-i(\phi_n - \omega_{n,n-1}\tau_n)\right] |J_{\max}\rangle.
\end{aligned}
\tag{S6}
$$

II.   MAXIMUM DEGREE OF ORIENTATION

We now provide further details regarding the theoretical maximum orientation. By utilizing the method of Lagrange multipliers, we can determine the maximum degree of orientation

$$
\mathcal{L}(c_0, c_1, \cdots, c_{J_{\max}}, \lambda) = f - \lambda g,
\tag{S7}
$$

where $J_{\max}$ represents the highest rotational state within the given subspace, the term

$$
f = 2 \sum_{J=0}^{J_{\max}-1} c_{J+1} c_J \mathcal{M}_{J+1,J}
\tag{S8}
$$

corresponds to the amplitude of the orientation at the full revivals, taking into account the relative phases in Eq. (6) in the main text to satisfy the relation $\varphi_{J+1,J} = (J + 1)\varphi_{1,0} + 2k\pi$, and λ is the Lagrange multiplier subject to a constraint of

$$
g = \sum_{J=0}^{J_{\max}} c_J^2 - 1 = 0
\tag{S9}
$$

To find the extremum of f subject to g, we can solve for the condition $\nabla \mathcal{L} = 0$, which leads to the following relations

$$\mathcal{M}_{1,0} c_1 - \lambda c_0 = 0,$$
$$\mathcal{M}_{1,0} c_0 + \mathcal{M}_{2,1} c_2 - \lambda c_1 = 0,$$
$$\mathcal{M}_{2,1} c_1 + \mathcal{M}_{3,2} c_3 - \lambda c_2 = 0, \tag{S10}$$
$$\cdots$$
$$\mathcal{M}_{J_{\max}, J_{\max}-1} c_{J_{\max}-1} - \lambda c_{J_{\max}} = 0.$$

By multiplying each equation in (S10) by the corresponding coefficients c_J of λ, we have

$$f - \lambda \left(\sum_{J=0}^{J_{\max}} c_J^2 \right) = f - \lambda = 0. \tag{S11}$$

The maximum degree of orientation, denoted by f, corresponds to the maximum value of λ determined by equation (S10). By examining the equations provided in Eq. (S10), we can derive the expansion coefficients

$$c_1 = \frac{\lambda}{\mathcal{M}_{1,0}} c_0,$$
$$c_2 = \frac{\lambda^2 - \mathcal{M}_{1,0}^2}{\mathcal{M}_{2,1} \mathcal{M}_{1,0}} c_0,$$
$$c_3 = \frac{\lambda^3 - (\mathcal{M}_{1,0}^2 + \mathcal{M}_{2,1}^2)\lambda}{\mathcal{M}_{3,2} \mathcal{M}_{2,1} \mathcal{M}_{1,0}} c_0, \tag{S12}$$
$$\cdots$$
$$c_{J_{\max}} = \frac{\lambda^{J_{\max}} + \sum_{k=1}^{[J_{\max}/2]} (-1)^k \left\{ \prod_{n=1}^{k} \sum_{l_1=0; l_n = l_{n-1}+2}^{J_{\max}-2k+2(n-1)} \mathcal{M}_{l_n+1,l_n}^2 \right\} \lambda^{J_{\max}-2k}}{\prod_{l=0}^{J_{\max}-1} \mathcal{M}_{l+1,l}^2} c_0,$$

where $[J_{\max}/2]$ equals to the greatest integer less than $J_{\max}/2$. Combining the last equation in Eq. (S10) with Eq. (S12), we have

$$\lambda^{J_{\max}+1} + \sum_{k=1}^{[\frac{J_{\max}+1}{2}]} (-1)^k \left\{ \prod_{n=1}^{k} \sum_{\substack{l_1=0; \\ l_n=l_{n-1}+2}}^{J_{\max}-1-2k+2n} \mathcal{M}_{l_n+1,l_n}^2 \right\} \lambda^{J_{\max}+1-2k} = 0. \tag{S13}$$

To obtain the maximum degree of orientation, we can solve Eq. (S13). Subsequently, the real positive amplitudes (c_J) of the rotational states can be found by substituting the obtained λ into Eq. (S12) and combining it with the condition $g = \sum_{J=0}^{J_{\max}} |c_J|^2 - 1 = 0$. By following this process, we can generate the desired rotational wave packet in the interaction picture

$$|\psi\rangle = \sum_{J=0}^{J_{\max}} c_J \exp(i\varphi_J) |J\rangle, \tag{S14}$$

4

where the optimal phases φ_J satisfy the relation $\varphi_{J+1} - \varphi_J = (J+1)(\varphi_1 - \varphi_0) + 2k\pi$.

Note that eigenvalue equations of the operator $\langle \cos\theta \rangle$ can only be solved analytically for simple two-level and three-level systems. As the complexity of the system increases, analytically finding eigenvalues and eigenvectors becomes challenging due to the intricacies involved in matrix diagonalization. Consequently, numerical methods such as Power Iteration, QR Algorithm, and Jacobi Method are commonly employed to determine eigenvalues and eigenvectors. This is the key reason why we solve Eq. (S13) instead of the eigenvalue equation to obtain the target wave packets. Table S1 lists the optimal population distributions of rotational states and the corresponding maximum degree of orientation for different $J_{\max}$.

III. AMPLITUDE AND PHASE CONDITIONS

Based on the above analysis, the maximum degree of orientation solved by Eq. (S13) requires that $\theta_j(t_f)$ satisfy the following relations:

$$\left| \cos\theta_1(t_f) \right| = c_0,$$

$$\left| i\sin\theta_1(t_f) \exp\left[-i(\phi_1 - \omega_{1,0}\tau_1)\right] \cos\theta_2(t_f) \right| = c_1,$$

$$\cdots \tag{S15}$$

$$\left| \prod_{n=1}^{N} i\sin\theta_n(t_f) \exp\left[-i(\phi_n - \omega_{n,n-1}\tau_n)\right] \right| = c_{J_{\max}},$$

and

$$\varphi_{J+1,J} = \varphi_{J+1} - \varphi_J = \frac{\pi}{2} - \phi_{J+1} + \omega_{J+1,J}\tau_{J+1},$$

$$\varphi_{1,0} = \varphi_1 - \varphi_0 = \frac{\pi}{2} - \phi_1 + \omega_{1,0}\tau_1. \tag{S16}$$

By solving the equations in (S15), we can obtain the amplitude conditions for generating the maximum degree of orientation, i.e.,

$$\begin{cases} \theta_1(t_f) = \arccos c_0, \\ \theta_n(t_f) = \arccos \frac{c_{n-1}}{\left| \prod_{k=1}^{n-1} i\sin\theta_k(t_f) \exp\left[-i(\phi_k - \omega_{k,k-1}\tau_k)\right] \right|}, \quad (1 < n \le N). \end{cases} \tag{S17}$$

Furthermore, according to Eq. (S16) and the relation $\varphi_{J+1} - \varphi_J = (J+1)(\varphi_1 - \varphi_0) + 2k\pi$, the complex pulse areas $\theta_n(t_f)$ are also required to meet the phase condition

$$\phi_n = \omega_{n,n-1}\tau_n - n(-\phi_1 + \omega_{1,0}\tau_1) - \frac{(n-1)\pi}{2} + 2k\pi, \quad (n > 1). \tag{S18}$$

TABLE S1. The maximum degree of orientation and the corresponding population distributions $|c_J|^2$ of rotational states for a given value of J_{max}.

J_{max}	$\langle\cos\theta\rangle_{max}$	P_0	P_1	P_2	P_3	P_4	P_5	P_6	P_7	P_8	P_9	P_{10}	P_{11}	P_{12}	P_{13}	P_{14}	P_{15}
1	0.577	0.5	0.5														
2	0.775	0.278	0.5	0.222													
3	0.861	0.174	0.387	0.326	0.113												
4	0.906	0.119	0.292	0.317	0.208	0.064											
5	0.933	0.086	0.223	0.277	0.237	0.137	0.040										
6	0.949	0.065	0.175	0.235	0.231	0.174	0.094	0.026									
7	0.960	0.051	0.140	0.197	0.212	0.185	0.130	0.067	0.018								
8	0.968	0.041	0.114	0.167	0.190	0.181	0.147	0.098	0.049	0.013							
9	0.974	0.033	0.095	0.142	0.168	0.171	0.152	0.117	0.076	0.037	0.010						
10	0.978	0.028	0.080	0.122	0.149	0.157	0.149	0.126	0.126	0.059	0.029	0.008					
11	0.982	0.024	0.068	0.105	0.131	0.144	0.142	0.128	0.105	0.076	0.047	0.047	0.006				
12	0.984	0.020	0.020	0.092	0.117	0.131	0.134	0.127	0.110	0.088	0.063	0.038	0.018	0.005			
13	0.986	0.018	0.051	0.081	0.104	0.119	0.125	0.122	0.111	0.095	0.074	0.074	0.031	0.015	0.004		
14	0.988	0.015	0.045	0.072	0.093	0.108	0.116	0.116	0.110	0.098	0.081	0.062	0.043	0.026	0.012	0.003	
15	0.990	0.014	0.040	0.064	0.084	0.098	0.107	0.110	0.107	0.098	0.086	0.070	0.053	0.037	0.022	0.010	0.003

6

IV. ADDITIONAL SIMULATIONS

The control scheme proposed in this scenario involves implementing a pure rotational ladder-climbing excitation to achieve the desired superposition of rotational states and maximize the degree of orientation. To investigate the suitable bandwidth regime for the pulse sequence, we consider the case where J_{max} = 15 and assume that all sub-pulses have the same bandwidth, denoted as $\Delta\omega_n = \Delta\omega$. The amplitude of the sub-pulses follows Eq. (S17), and the center time of the nth sub-pulse is fixed at $\tau_n = 5(n-1)T_n$ to satisfy the phase condition stated in Eq. (S18).
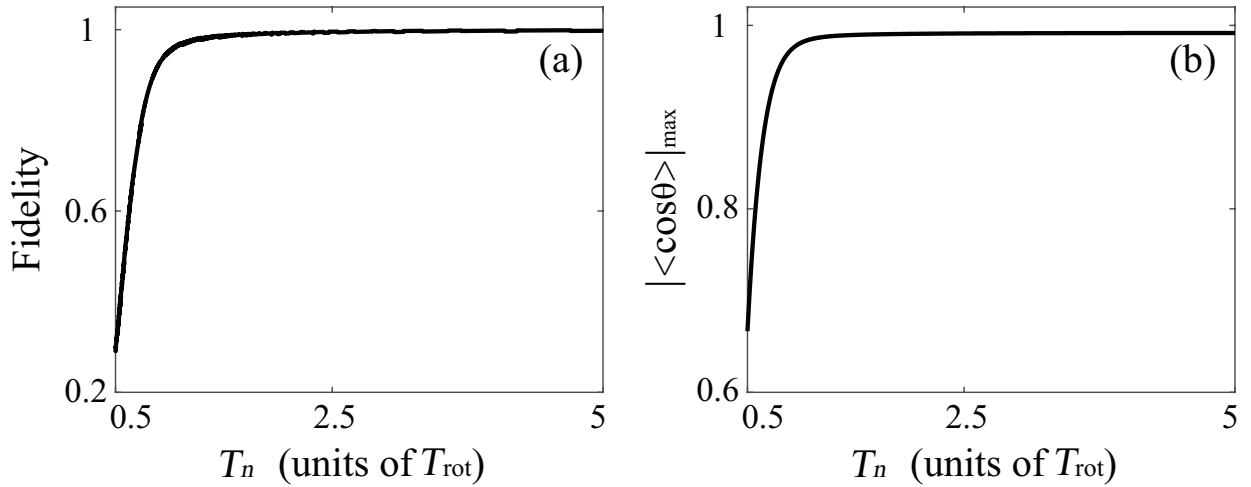
FIG. S1. Numerical simulations by utilizing the pulse sequence in Eq. (5) with N = 15. The (a) fidelity and (b) maximum orientation values $|\langle\cos\theta\rangle|_{max}$ are shown vs the bandwidth of the pulses, where $T_n = 1/\Delta\omega$.

Figure S1 displays the dependence of the fidelity $F = \langle\psi(t_f)|\psi\rangle\langle\psi|\psi(t_f)\rangle$ and the corresponding maximum orientation values on the bandwidth $\Delta\omega$. We can observe that the fidelity consistently remains high over 0.99 for durations of $T_n > T_{rot}$, indicating that each excitation period can be as short as the rotational period. In the narrow-bandwidth regime, the fidelity can reach high values of $F > 0.997$, resulting in theoretical maximum orientation values. In the broad bandwidth regimes, however, the fidelity decreases and the corresponding orientation value decreases. To this end, we perform all simulations by considering the pulse sequences in the narrow bandwidth regime with the duration of $T_n = 3T_{rot}$.

As can be seen from our derivation, the fidelity and maximum orientation depend on the area of each sub-pulse, a product of the dipole moment and the electric field strength. Therefore, it is not necessary to accurately determine the value of the dipole moment, as the pulse area condition
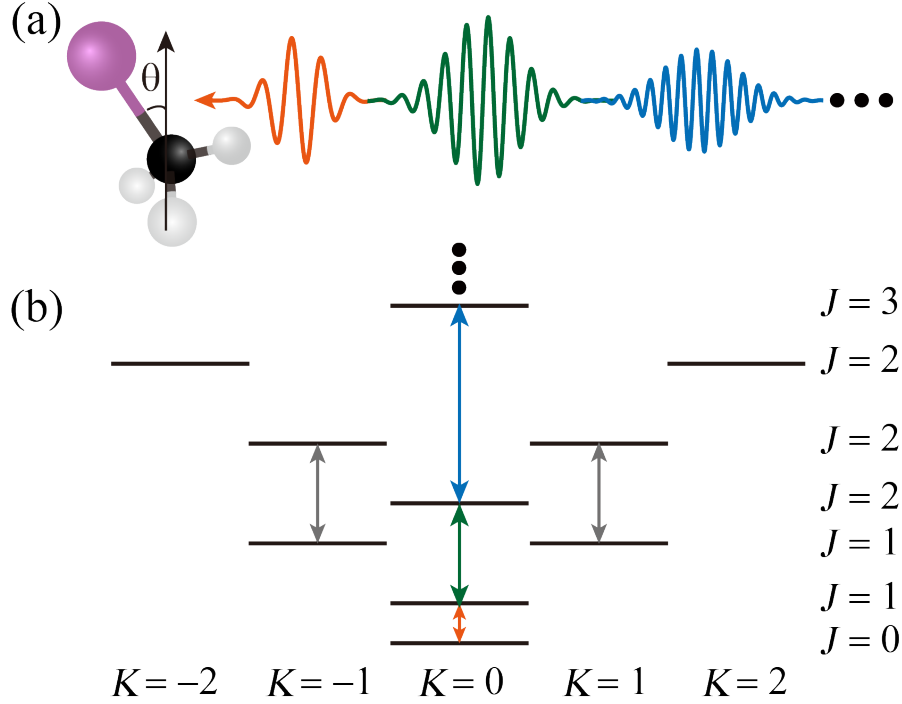
7

FIG. S2. The application of the analytical method to the polyatomic molecule (CH_3I). (a) Schematic representation of an ultracold symmetric-top molecule subjected to a pulse sequence, and (b) the corresponding energy level diagram. θ denotes the angle between the molecular symmetry axis and the field polarization direction.

can be met by controlling the field strength of the sub-pulse. It is indicated that fluctuations in the field strength affect the experimental precision. For the pulse with $T_n = 6.6$ ps used in the simulations, if the field strength fluctuation can be controlled to less than 3%, the fidelity can still be maintained at a high value over 0.99. This requirement is not strict for the current precision spectroscopy techniques.

It is well known that the stability of the carrier wave frequency and phase directly affects the performance and accuracy of microwave pulses in various applications, especially in precision spectroscopy, quantum computing, and communication systems. Our proposed theoretical scheme does necessitate precise terahertz and microwave shaping techniques. For our utilized pulses with a duration of $T_n = 6.6$ ps, in order to maintain fidelity above 0.99, frequency-detuning fluctuations should be controlled to less than 1‰, and pulse phase fluctuations should be kept below 6%.

V. APPLICATIONS TO POLYATOMIC MOLECULES

We now demonstrate the generalization of applying our analytical method to polyatomic molecules. By considering pure rotational excitation in its absolute ground state, the field-free Hamiltonian of the polyatomic nonlinear molecule can be given by

$$\hat{H}_0 = A\hat{J}_a^2 + B\hat{J}_b^2 + C\hat{J}_c^2, \tag{S19}$$

where $\hat{J}_a$, $\hat{J}_b$, and $\hat{J}_c$ represent the angular momentum operators concerning the principal molecular axes, and $A > B > C$ are the rotational constants. Based on the relations of rotational constants, polyatomic molecules can be classified as asymmetric-top ($A > B > C$), symmetric-top (oblate $A = B > C$ or prolate $A > B = C$), spherical-top ($A = B = C$), or linear-top ($A = B, C = 0$) [1]. Our analytical approach can be directly applied to all symmetric types of polyatomic molecules, except for asymmetric top molecules, which require suitable adjustments in the amplitudes and center frequencies of subpulses.

As an example, we examine how to apply the present analytical method to prolate symmetric-top molecules ($A > B = C$) in Fig. S2(a). The corresponding Hamiltonian can be written as

$$\hat{H}_s = C\hat{J}^2 + (A - C)\hat{J}_z^2, \tag{S20}$$

where we assign the axes as $a \rightarrow z$, $b \rightarrow x$, and $c \rightarrow y$ in the molecular fixed frame. The eigenfunctions $|JKM\rangle$ satisfy

$$\hat{H}_s |JKM\rangle = E_{JK} |JKM\rangle, \tag{S21}$$

where the eigenenergies $E_{JK} = CJ(J + 1) + (A - C)K^2$ are associated with the quantum numbers J ($J = 0, 1, 2, ...$), and M and K ($M, K = -J, -J + 1, ..., J$). The latter describes rotation relative to a space-fixed axis and a molecule-fixed axis, respectively. The interaction between the molecule and linearly polarized pulses is given by

$$\hat{H}_\mu(t) = -\mu_0 D_{00}^1 E(t) = -\mu_0 \cos\theta E(t), \tag{S22}$$

where θ denotes the angle between the molecular symmetry axis and the field polarization direction, and μ_0 represents the permanent dipole moment. By using Wigner 3j-symbols or Clebsch-Gordan coefficients, the dipole transition matrix elements between rotational states can be ex-

pressed as follows [2, 3]

$$\langle J''K''M''|D^J_{MK}|J'K'M'\rangle = \sqrt{2J''+1}\sqrt{2J'+1}(-1)^{M''+K''}\begin{pmatrix} J' & J & J'' \\ M' & M & -M'' \end{pmatrix}\begin{pmatrix} J' & J & J'' \\ K' & K & -K'' \end{pmatrix} \quad (S23)$$

$$= \sqrt{2J'+1}/\sqrt{2J''+1}\,\langle J'M'JM|J''M''\rangle\langle J'K'JK|J''K''\rangle,$$

which govern the selection rules $\Delta J = \pm 1$, $\Delta K = 0$, and $\Delta M = 0$, as shown in Fig. S2(b).

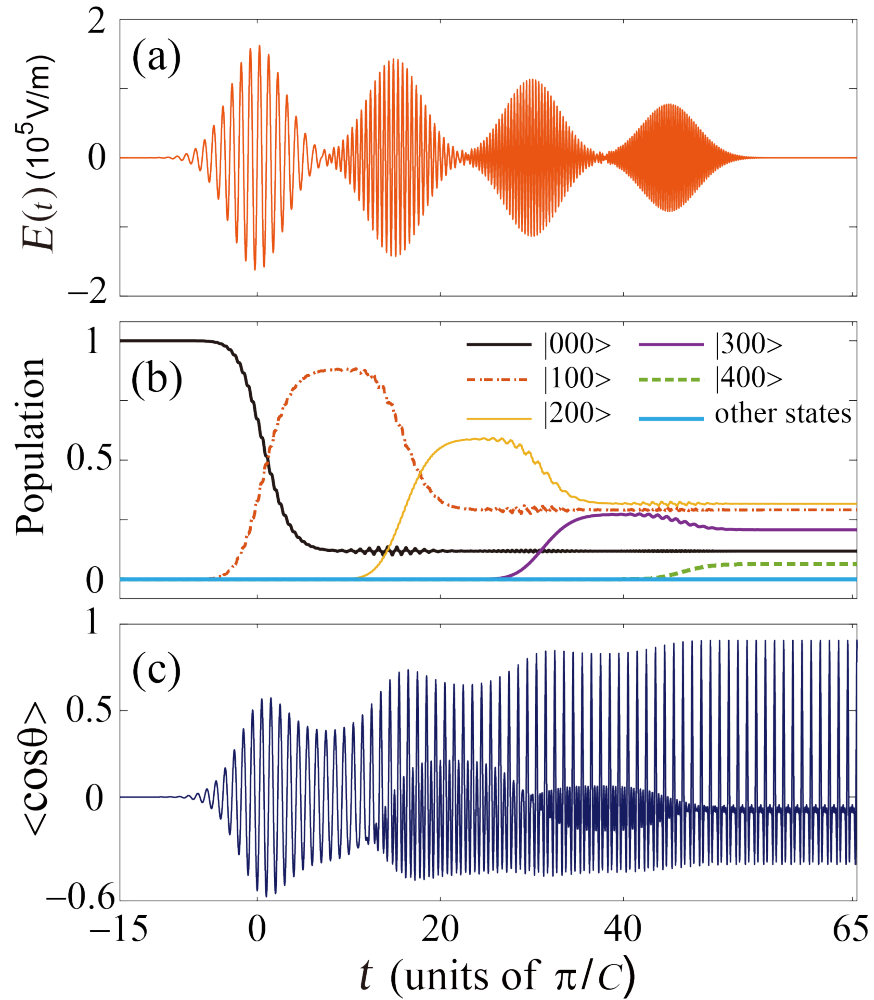By considering the molecule initially in a pure rotational state $|J_0K_0M_0\rangle$, the time-dependent

FIG. S3. Simulations for the application of the analytical method to the polyatomic molecule (CH_3I). (a) The time-dependent electric field of the pulse sequence consisting of four optimal sub-pulses, (b) the corresponding time-dependent populations of the rotational states, and (c) the corresponding field-free molecular orientation evolution. The time is measured in units of the full revival period $\pi/C = 66.5$ ps of the molecule.

wave function after rotational excitation can be expanded as

$$\left|\psi_{J_0 K_0 M_0}(t)\right\rangle = \sum_{J=J_i}^{J_{max}} c_{JK_0 M_0}(t) e^{i\varphi_{JK_0 M_0}} e^{-iE_{JK_0}t} \left|JK_0 M_0\right\rangle, \tag{S24}$$

where $J_i = \max\{|K_0|, |M_0|\}$. $c_{JK_0 M}(t)$ and $\varphi_{JK_0 M}$ represent the real positive amplitude and phase of the rotational state $|JK_0 M\rangle$, determined by $c_{JK_0 M}(t) e^{i\varphi_{JK_0 M}} = \langle JK_0 M| \hat{U}(t, t_0) |J_0 K_0 M_0\rangle$. The degree of orientation for the symmetric-top molecules can be given by

$$\begin{aligned}
\langle\cos\theta\rangle(t) &= \left\langle\psi_{J_0 K_0 M_0}(t)\right| \cos\theta \left|\psi_{J_0 K_0 M_0}(t)\right\rangle \\
&= \sum_{J=J_i}^{J_{max}} c_{JK_0 M_0}(t)^2 \mathcal{N}_{J,J} + 2 \sum_{J=J_i}^{J_{max}-1} c_{JK_0 M_0}(t) c_{J+1K_0 M_0}(t) \\
&\quad \times \mathcal{N}_{J+1,J} \cos(\omega'_{J+1,J}t - \varphi'_{J+1,J}).
\end{aligned} \tag{S25}$$

where

$$\begin{aligned}
\mathcal{N}_{J,J} &= \langle JK_0 M_0| \cos\theta |JK_0 M_0\rangle = \frac{K_0 M_0}{J(J+1)}, \\
\mathcal{N}_{J+1,J} &= \langle J+1K_0 M_0| \cos\theta |JK_0 M_0\rangle = \frac{\sqrt{(J+1)^2 - K_0^2}\sqrt{(J+1)^2 - M_0^2}}{(J+1)\sqrt{(2J+1)(2J+3)}},
\end{aligned} \tag{S26}$$

where the transition frequencies are defined by $\omega'_{J+1,J} = E_{J+1K_0} - E_{JK_0}$, and the relative phases are $\varphi'_{J+1,J} = \varphi'_{J+1K_0 M_0} - \varphi'_{JK_0 M_0}$. For the absolute ground state $|J_0 = 0, K_0 = 0, M_0 = 0\rangle$, the degree of orientation described by Eq. (S25) is exactly the same as for the diatomic molecule in Eq. (6) of the main text. This indicates that the maximum orientation of the symmetric-top molecules and the corresponding population distributions align with those listed in Table S1. Furthermore, it is clear that the optimal pulse sequence obtained in Eq. (5) in the main text can generate the desired orientation values for the symmetric top molecules.

To confirm this point and to visualize the time-dependent population evolutions clearly, we apply an optimal pulse sequence consisting of four sub-pulses to a polyatomic molecule (CH_3I) with $A = 5.173949\text{cm}^{-1}$, $C = 0.25098\text{cm}^{-1}$, and $\mu_0 = 1.6406\text{D}$ [4]. Figure S3 displays the optimal pulse sequence, the corresponding field-free orientation evolution, and the time-dependent populations of rotational states. As expected, the optimal pulse sequence in Fig. S3(a) results in a maximum orientation value of 0.906 in Fig. S3(b). It also leads to optimal population distributions across the five desired rotational states while keeping other unwanted rotational states unpopulated in Fig. S3(c). Interestingly, the optimal pulse sequence is obtained by scaling only the center frequencies and amplitudes of the pulses utilized for LiH molecules with the rotational constant C and the dipole moment μ_0 of CH_3I. This means that the electric field strengths of all sub-pulses in

11

Fig. S3(a) are reduced by a constant of 8.4 in comparison to the pulses applied for LiH molecules in Fig. 2(c) of the main text. By applying more optimal sub-pulses to the system, we can attain enhanced molecular orientations.

Further analysis of the asymmetric top molecule indicates that by using three rotational constants (A, B and C) and three dipole moments (μ_a, μ_b and μ_c) to determine the central frequencies and amplitudes of sub-pulses, this analytical method can be extended to asymmetric top molecules starting from the absolute ground state ($v = 0$ and $J = 0$), leading to desired three-dimensional molecular orientations.

---

[1] C. P. Koch, M. Lemeshko, and D. Sugny, Quantum control of molecular rotation, Rev. Mod. Phys. **91**, 035005 (2019).

[2] M. Leibscher, T. F. Giesen, and C. P. Koch, Principles of enantio-selective excitation in three-wave mixing spectroscopy of chiral molecules, J. Chem. Phys. **151** (2019).

[3] A. B. Magann, T.-S. Ho, C. Arenz, and H. A. Rabitz, Quantum tracking control of the orientation of symmetric-top molecules, Phys. Rev. A **108**, 033106 (2023).

[4] P. Babilotte, K. Hamraoui, F. Billard, E. Hertz, B. Lavorel, O. Faucher, and D. Sugny, Observation of the field-free orientation of a symmetric-top molecule by terahertz laser pulses at high temperature, Phys. Rev. A **94**, 043403 (2016).